Transcriptome dynamics of *Pseudomonas aeruginosa* during transition from replication-uncoupled to -coupled growth

Kathrin Alpers[1], Elisabeth Vatareck[1], Lothar Gröbe[2], Mathias Müsken[3], Maren Scharfe[4], Susanne Häussler[1,5,6,7*], Jürgen Tomasch[1,8*]

[1]Department of Molecular Bacteriology, Helmholtz Centre for Infection Research, Braunschweig, Germany
[2]Platform Flow Cytometry and Cell Sorting, Department of Experimental Immunology, Helmholtz Centre for Infection Research, Braunschweig, Germany
[3]Central Facility for Microscopy, Helmholtz Centre for Infection Research, Braunschweig, Germany
[4]Platform Genome Analytics, Helmholtz Centre for Infection Research, Braunschweig, Germany
[5]Institute for Molecular Bacteriology, Twincore, Centre for Clinical and Experimental Infection Research, Hannover, Germany
[6]Department of Clinical Microbiology, Copenhagen University Hospital – Rigshospitalet, 2100 Copenhagen, Denmark
[7]Cluster of Excellence RESIST (EXC 2155), Hannover Medical School, 30265 Hannover, Germany
[8]Institute of Microbiology of the Czech Academy of Science, Center Algatech, Třeboň, Czech Republic

*correspondence: Susanne.Haeussler@helmholtz-hzi.de
*correspondence: tomasch@alga.cz

Abstract

In bacteria, either chromosome duplication is coupled to cell division with only one replication round per cell cycle or DNA is replicated faster than the cells divide thus both processes are uncoupled. Here, we show that the opportunistic pathogen *Pseudomonas aeruginosa* switches from fast uncoupled to sustained coupled growth when cultivated under standard laboratory conditions. The transition was characterized by fast-paced, sequential changes in transcriptional activity along the *ori-ter* axis of the chromosome reflecting adaptation to the metabolic needs during both growth phases. Quorum sensing (QS) activity was highest at the onset of the coupled growth phase during which only a quarter of the cells keeps replicating. RNA sequencing of subpopulations of these cultures sorted based on their DNA content, revealed a strong gene dosage effect as well as specific expression patterns for replicating and non-replicating cells. Expression of flagella and *mexE*, involved in multi drug efflux was restricted to cells that did not replicate, while those that did showed a high activity of the cell division locus and recombination genes. A possible role of QS in the formation of these subpopulations upon switching to coupled growth could be a subject of further research.

Significance statement

The coordination of gene expression with the cell cycle has so far been studied only in a handful of bacteria, the bottleneck being the need for synchronized cultures. Here, we determined replication-associated effects on transcription by comparing *Pseudomonas aeruginosa* cultures that differ in their growth mode and number of replicating chromosomes. We further show that cell cycle-specific gene regulation can be principally identified by RNA sequencing of subpopulations from cultures that replicate only once per cell division and that are sorted according to their DNA content. Our approach opens the possibility to study asynchronously growing bacteria from a wide phylogenetic range and thereby enhance our understanding of the evolution of cell-cycle control on the transcriptional level.

Introduction

Bacteria differ in the ways replication is coordinated with cell growth and division[1]. In fast-growing representatives, such as the model organisms *Escherichia coli* or *Bacillus subtilis*, the speed of DNA replication exceeds that of cell division. This uncoupling of both processes results in a gene dosage gradient along the origin(*ori*)-terminus(*ter*) axis of the chromosome. The higher gene copy number closer to *ori* can be exploited to maximize expression of traits needed during rapid growth and to control gene expression[2,3]. It has been shown that moving an *ori*-located *Vibrio cholerae* gene cluster coding for ribosomal proteins close to *ter* reduced the growth rate of the culture, while the wild-type growth level could be restored by placing two copies of this cluster at *ter*[4]. Furthermore, the timing of spore formation in *B. subtilis* is an example for dosage imbalances triggering regulatory events between genes located on opposite ends of the replicating chromosomes[5]. In slow-growing bacteria the chromosome is duplicated only once per cell division, thus both processes are coupled[6]. In several bacterial phyla, a differentiation program is triggered during this eukaryote-like cell cycle. The best studied model is the bi-phasic lifestyle of *Caulobacter crescentus*. In this bacterium a complex gene regulatory network precisely times the development of a flagellated from a stalked cell during replication and cell division[7].

Pseudomonas aeruginosa is a ubiquitous environmental bacterium, but also an opportunistic pathogen frequently causing nosocomial infections of various body sites, such as the lung, bloodstream, urinary tract and burn wounds[8]. Furthermore, *P. aeruginosa* poses a particular threat to patients suffering from cystic fibrosis (CF)[9]. During live-long chronic infections of the CF lung, the bacterium adapts and evolves towards a slow growing phenotype[10]. Doubling times are estimated to be around 30 min under laboratory conditions in lysogeny broth (LB) medium and 1.9 to 4.6 h in the CF lung[11]. The cell cycle dynamics of *P. aeruginosa* has been extensively studied. Its chromosome is oriented with *ori* close to the center of the cell and *ter* located at the cell pole where the division plane forms. During replication both *ori* move to the poles of the elongated pre-divisional cell where another round of replication can be started[12,13]. Despite the huge body of comparative transcriptome data available for this important pathogen[14–16], the effect of replication on gene expression has not explicitly been studied yet.

Here we monitored growth and cell division and recorded a time-resolved transcriptome of *P. aeruginosa* PA14 in LB medium over 10 hours at 1 hour intervals. We show that the culture switches from fast replication-uncoupled to sustained coupled growth. The transition is characterized by fast-paced, sequential changes in transcriptional activity along the *ori-ter* axis. Furthermore, we identified replication- and non-replication-associated gene expression in cells showing coupled growth using a newly developed protocol based on fluorescence-activated cell sorting (FACS).

Results

Growth and replication dynamics of *P. aeruginosa* in LB medium.

In accordance with previous reports[11], *P. aeruginosa* cultures reached an OD_{600} of 1.8±0.24 from a starting OD_{600} of 0.05 within 4 h and a maximum doubling time of 34±1 min when grown under standard laboratory conditions (Figure 1A). This exponential growth phase was followed by slower growth to a maximum OD_{600} of 3.17±0.11 after 9 h with an OD value doubling time of 410±110 min. Cell numbers, too, increased exponentially in the first four hours from $4.5*10^7$ to $7.3*10^8 \pm 1.8*10^8$ cells/ml with a doubling time of 30±9 min, followed by decreased growth to a maximum count of $3.7*10^9 \pm 5.8*10^7$ cells/ml after 9 h with a doubling time of 168±6 min. The notably slower increase of OD_{600} values compared to cell numbers in the last 6 h of cultivation could be explained by a decrease in cell size at later growth stages that is indicative for reductive cell division (Figure 1B, Supplementary Figure S1A).

The chromosome content of cells was monitored by stoichiometric staining with SYBR Green (Figure 1C, Supplementary Figure S1B). In the over-night grown pre-cultures that were used for inoculation, 80% of the cells contained one chromosome (C1). One hour after the transfer into fresh medium already 62±7% and 30±2% of the cells contained two (C2) and three chromosome equivalents, respectively, and a smaller fraction even more. This clearly indicates that the cultures had moved to a phase of uncoupled growth with replication being faster than cell division. After 4 to 5 h of growth, the chromosome content shifted back and two distinct peaks for cells containing one or two chromosomes became visible again. The presence of cells with a DNA content between the major peaks indicates actively replicating cells (R). The proportion of C2 and R cells was only slowly reduced from 38±3% to 23±2% between 6 h and 10 h of growth. The presence of replicating cells after 10 h of cultivation

was also visible on electron micrographs (Figure 1D). Our data strongly suggest that *P. aeruginosa* shifts from fast uncoupled to sustained coupled growth cells during the course of cultivation in LB medium with a short transition phase in between (Figure 1C). If the doubling time of the coupled growing culture is converted to the approximately 25% of cells that actually replicate, the individual division times are around 42 min, thus only slightly lower than in the uncoupled growth phase.

Transcriptome dynamics of *P. aeruginosa* during different growth phases.

We monitored transcriptional changes for the full growth period in one-hour intervals. Two independent experiments with two and three replicates each were carried out. The transcriptomes clustered according to the growth phases except for the 6 h samples. For these samples, the transcriptomes of the first experiment were closer to the transition phase, while the transcriptomes of the second experiment were closer to the coupled growth phase samples (Supplementary Figure S2A). The 1736 genes, which showed a significant differential expression during the course of cultivation, could be assigned to eight clusters (Supplementary Figure S2B and C and Supplementary Table S1).

The transition between growth-phases was characterized by fast-paced waves of transient transcriptional activity (Figure 2A). Genes in clusters 1 to 3 showed a comparable high expression during the first 2 h of uncoupled growth, but with a different timing of maximum expression and the decline afterwards. During this growth phase, in particular transcription and translation-related processes were expressed (Figure 2B), including biosynthesis of tRNAs, RNA polymerase and ribosomes as well as chaperones. A high activity was seen for oxidative phosphorylation and also for biosynthesis of the vitamins folate (B9) and cobalamin (B12), in accordance with their respective roles in DNA and methionine synthesis. Expression of the type III secretion system gene clusters *psc* and *pcr* and the *exoT* effector [17] peaked at 2 h of cultivation followed by a steep decline.

Cluster 4 to 6 contained genes that were transiently activated at the end of exponential growth. The high number of sugar and amino acid transporters as well as genes of the pyruvate metabolism indicated a shift in the metabolic preferences. In particular transporters for branched-chain amino acids were found to be upregulated in this transition phase, in accordance with their late utilization as a carbon source observed before[10]. Activation of the urea cycle and denitrification, and the glycogen metabolism pathway indicate changes of

nitrogen and carbon utilization at this stage. Cluster 7 harbored genes, which were activated late in the transition phase and exhibited a stable expression throughout the coupled growth phase. Denitrification genes were among them as well as genes encoding subunits of a sulfate transporter and the MexHIG antibiotic efflux pump[18]. Finally, expression of the late responding genes in cluster 8 increased between 5 and 8 h before reaching a stable level. In particular, activation of the pyoverdine biosynthesis machinery, the heme acquisition protein HasA and the sulfonate transport and metabolism pathway indicate a response to iron and sulfur limitation in the medium, respectively.

The three components of the quorum sensing system showed different activation dynamics consistent with previous data[19,20]. While the primary QS activator *lasR*/*rsaL* pair was not among the significantly regulated genes, its expression showed a small but consistent gradually increase from 2 h cultivation on (Supplementary Table S1). The *pqsABCDE*-operon was transiently activated with a peak between 4 and 5 h followed by a decline and therefore found in cluster 5. The pyocyanin biosynthesis gene clusters showed the same pattern, but with a much more pronounced peak. The chemotaxis operon was also activated transiently during in the transition phase (cluster 6), while flagella genes were not differentially regulated. The QS regulator RhlR was assigned to cluster 7 with an activation delay but stable expression throughout coupled growth. The QS target genes coding for alkaline protease, cyanide production and lectin B were found in the same cluster.

Influence of gene dosage on the transcriptome during uncoupled growth.

Next, we analyzed the distribution of genes in the determined clusters along the *ori*-*ter*-axis of the chromosome. Genes active during uncoupled growth (clusters 1 to 3) were predominantly located close to *ori* while those that were activated during the transition phase (clusters 4 and 5) were more equally distributed along the chromosome. Genes in cluster 6, activated at the end of the transition phase, already showed a tendency towards *ter*, a trend that became even more pronounced for the genes in clusters 7 and 8 that increased expression during coupled growth (Figure 3A). Furthermore, the average expression levels of genes in the *ori*-proximal half exceeded those in the *ter*-proximal half of the chromosome during the first three hours of uncoupled growth. At later time-points a balanced expression of both halves of the chromosome was observed (Figure 3B). These data are in accordance with the predicted gene dosage effect in cells with high replication rates.

The gene dosage effect became also visible when a general additive model was fitted to the $\log_2$ fold-change transcriptome data along the chromosome in order to identify local trends in expression dynamics that go beyond the regulation of single genes or operons. When comparing subsequent time-points, with a gradual change in chromosome content, a slightly lower expression was found around the terminus when transcriptomes from 3 h versus 4 h were compared (and to a lesser extent for 2 h vs. 3 h, Supplementary Figure S3). This comparison marks the beginning of the transition from uncoupled to coupled growth and also showed the strongest shift in chromosome content during cultivation.

The position-specific differences in gene expression became more pronounced when we compared transcriptomes of time-points with a higher difference in chromosome content (Figure 3C). A clearly lower transcription of genes in the region surrounding the terminus of replication was visible when the different growth phases were compared, in particular seen for uncoupled versus coupled growth. To a lesser extent this trend was also seen for the comparison of uncoupled growth to transition and transition to coupled growth phase. In accordance with the analysis above, this specific reduction of gene expression proximal to, and also increasing towards *ter*, can be parsimoniously explained by a change in mRNA composition as a result of a higher transcriptional activity of *ori*-proximal genes, thus a gene-dosage effect (indicated by the orange line in Figure 3C).

Replication-associated transcriptome changes during coupled growth.

The coupled growth with only one replication per cell division in the last 6 hours of cultivation should allow to discriminate the transcriptomes of non-replicating, replicating and pre-divisional *P. aeruginosa* cells. To this end, we developed a protocol employing FACS to separate cells based on their chromosome content (Supplementary Text S1). In order to determine the influence of fixation with formaldehyde (FA), and FACS on RNA composition, we compared samples obtained during different steps of the protocol to a sample fixed with RNAprotect (RP) (Figure 4A). Across the three replicates, the different samples showed a consistently high correlation (Figure 4B, Supplementary Figure 4A). We only found 15 genes as well as the chromosomal region of 32 phage-related genes, which were higher expressed in the RP- than in the FA-treated samples (Supplementary Table S2). Only two genes found to be regulated during the cell cycle were also influenced by the fixation method, thus rendering the protocol suitable for the intended purpose.

Next we compared the transcriptomes of the cell populations with one (C1) or two (C2) chromosomes and those replicating (R). The R and C2 fractions differed from the C1 fraction, but were highly similar to each other (Figure 4C). Only eleven genes were found to be differentially expressed exclusively when these two fractions were compared. This included the *gnyDBHAL* gene cluster coding for enzymes of the acyclic isoprenoid degradation pathway[21], which showed the strongest downregulation in the R versus C2 fraction. The *nrdAB* genes coding for both subunits of the ribonucleotide-diphosphate reductase were downregulated in the C2 fraction compared to C1 and R. This enzyme catalyzes the last step in the formation of deoxyribonucleotides. In *E. coli*, it is activity has been linked to controlling the rate of DNA synthesis[22]. Furthermore, it has been shown that gene expression peaks at initiation and declines towards the end of replication which is in accordance with our data for *P. aeruginosa*.

Between the actively replicating R and the C1 fraction, a clear dosage effect was visible with gene expression decreasing from *ori* to *ter* (Figure 4D). The same was seen for the comparison of R and C2, but not when the fractions with only completely replicated chromosomes, C1 and C2 were compared (Supplementary Figure S4B). The differential expression of several chromosomal loci exceeded this trend dependent on the chromosomal position. In the R (and C2) fraction, the genes encoding the divisome showed the strongest activation compared to C1. These comprise of the *mur* and *mra* operons, encoding the enzymes for remodeling the peptidoglycan layer at the division plane and the *fts* genes, encoding the components responsible for septum formation[23]. The recombination genes *lexA* and *recG* were upregulated, too. Of note was also the transcriptional activation of one genomic island, the region of genomic plasticity RGP41[24], consisting of only uncharacterized genes. In the C1 fraction, the flagella gene clusters and chemotaxis operons, as well as the *glg* genes encoding the enzymes of the glycogen metabolic pathway showed the strongest activation compared to R and C2. Notably, the *mexE* gene, completely inactive in the other fractions, also showed a more than 64-fold higher expression in the C1 population, by far the strongest regulation in the dataset (Supplementary Table S2). It encodes the transmembrane protein part of an efflux-transporter for norfloxacin and imipenem[18].

Discussion

Here we showed that *P. aeruginosa* switches from replication-uncoupled to -coupled growth when cultivated in LB medium, thus allowing to study the effect of replication on the transcriptome. Hereby, the chromosomal gene order reflects the expression maxima during both growth-phases with the genes important for fast uncoupled growth being located closer to *ori* and the stationary phase genes located closer to *ter*. It has been demonstrated before that the *E. coli* sigma 70 factor and its targets, which are mostly active in the exponential phase, are located closer to *ori,* while the sigma S factor and its mostly stationary phase active targets are located closer to *ter*[25]. Thus, while the sigma factors transcriptionally regulate downstream genes, regulon expression is additionally enhanced by a gene dosage effect acting on the regulators and their target genes. Our data show the potential of combining identification of different growth phases by flow cytometry with the comparison of the respective transcriptomes. The gained knowledge could generally be used to identify replication-associated effects on gene expression for the vast number of strains with existing transcriptome data[14,16,26], and integrated into existing gene regulatory models[15,27]. It could further help to better understand chromosomal architecture and to explain gene order evolution[2,25,28,29].

In the coupled growth phase, *P. aeruginosa* displays a distinct transcriptome between the approx. 25% dividing and 75% non-dividing cells. Expression of flagella genes is restricted to cells that are not replicating, while those that replicate differ mainly in the activity of a cell division locus. Furthermore, we found that expression of *mexE*, involved in the expression of an important antibiotic resistance trait is restricted to the non-dividing cells. This induction of subpopulations during the switch in growth phases is coincidental with the activation of the *rhl* QS system. Cell communication induced population heterogeneity has been shown for *P. aeruginosa* before[30] and is also common in other bacteria[31–33]. It might also be the trigger switching the replication mode and restricting activity of the flagella gene clusters to the non-dividing cells. In contrast to chemotaxis, flagella gene expression has not been described to be controlled directly by QS before[19,20]. However, we also did not find them differentially expressed in the culture as a whole, but only in a subpopulation. Thus, a possible connection between communication and development of motility in a fraction of cells might have been overlooked and is worth a closer investigation. Furthermore, slow-growing QS-defective mutants frequently evolve during CF infections[34,35] It would be interesting to determine if

these strains reproduce by coupled growth only and how the transcriptome is affected by this change.

The highly similar transcriptomes of replicating and pre-divisional cells indicate that in *P. aeruginosa* no distinct phases of a differentiation program are coupled to progressing replication. This is in stark contrast to the precisely timed cell cycle of *C. crescentus* with a defined order of gene activity as cells replicate[36]. Transcriptome dynamics during replication has so far only be determined for a couple of model bacteria[36–39]. Key to these studies was the ability to synchronize the cell cycle within the cultures. Our newly developed method based on cell sorting according to DNA content allows for identification of replication-specific gene expression without the need for synchronization, as long as the cells grow slowly with coupled replication and cell division. Not only cell sorting, but also complementary recent advances in single cell sequencing[40] open up the path to comparative analysis of larger groups of bacteria, thus contributing to a better understanding of the evolution of cell-cycle control at the transcriptional level[41].

Material and Methods

Strains and growth conditions.

Pseudomonas aeruginosa PA14[42] was grown in Lysogeny Broth (10 g/L tryptone, 5 g/L yeast extract, 10 g/L NaCl) at 37˚C and 160 rpm shaking. The growth of cultures inoculated to a starting OD_{600} of 0.05 was followed for 10h and samples for determination of OD_{600}, cell count, DNA content, and RNAseq were withdrawn every hour. For FACS-based sorting, cultures were inoculated to a starting OD_{600} of 0.2 and samples were prepared after 5 h when the coupled-growth mode was stably reached.

Flow cytometric determination of cell number and chromosome content.

100 µL of culture were mixed with 80 µL of 25% glutaraldehyde in H2O and incubated for 5 min. 820 µL of PBS were added and a dilution series up to 1:1000 was prepared. 10 µL of SYBR Green (100x) was added to 1 mL of diluted culture. After an incubation time of 20 min, the sample was measured on a BD FACS Canto flow cytometer (BD Biosciences, Heidelberg, Germany). After gating based on centered forward and sideward scatter, cells were identified and chromosome content quantified by fluorescence detection in the FITC

channel (excitation 488 and emission 535 nm). Data processing and analysis were performed with the R package ggcyto[43].

Electron microscopy.

Bacteria were fixed by addition of glutaraldehyde (final concentration 2%) for 30 minutes, and addition of formaldehyde (final concentration 5%) into the culture medium. EM sample preparation was performed as previously described[44] with slight modifications. In brief, samples were washed twice with TE-buffer and fixed to poly-l-lysine coated round cover slips. After additional washing steps, the samples were dehydrated in a gradient series of acetone (10%, 30%, 50%, 70%, 90%) on ice and two steps with 100% acetone at room temperature (each step for 10 minutes). Afterwards, samples were critically point dried with the CPD300 (Leica Microsystems, Wetzlar, Germany), mounted to aluminum pads and sputter coated with gold-palladium. Images were acquired with a field emission scanning electron microscope Merlin (Zeiss, Jena, Germany) equipped with an Everhart Thornley and an inlens detector and operating at an acceleration voltage of 5kV.

RNAseq library preparation from whole cultures.

Depending on the density, 1 to 2 mL of culture were mixed with the same volume RNAprotect™ Bacteria Reagent (Qiagen, Hilden, Germany) incubated for 10 min and centrifuged. The pellets were flash-frozen and stored at -70°C. RNA extraction was carried out with the RNeasy Plus Kit in combination with QIAshredder™ columns (Qiagen, Hilden, Germany). Treatment with DNase I was performed in solution. Multiplexed libraries were generated from directly barcoded fragmented RNA according to a previously published custom protocol[45], including rRNA removal with the RiboZero Kit (Illumina, San Diego, USA).

Fluorescence-activated cell sorting for RNAseq of subpopulations.

The method was developed based on a previously published study[46]. A step-by-step protocol for sample preparation, sorting and RNA isolation is provided in Supplementary Text S1. Key to successful RNA recovery is the gentle formaldehyde fixation at 4˚C. Aliquots of fixed samples were adjusted to approx. $1.8*10^7$ cells/mL in 30 ml volume each and stained with SYBR Green. Sorting of $5.4*10^8$ cells based on the FITC-signal (see above) directly into RNAprotect was performed with the BD FACSAria Fusion (BD Biosciences, Heidelberg, Germany). The sorted cells were collected on a filter from which RNA was extracted using a

combination of Lysozyme and Proteinase K digestion with bead beating, and purified with NucleoZOL (Takara Bio, Göteborg, Sweden). Ribosomal RNA depletion was performed with the NEBNext Bacteria kit (NEB, Frankfurt, Germany). The libraries were prepared with the TruSeq kit (Illumina, San Diego USA).

Transcriptome analysis

Sequencing of all libraries was performed on a NovaSeq 6000 (Illumina, San Diego, USA) in paired-end mode with 100 cycles in total. Reads were filtered with fastQC-mcf (https://github.com/ExpressionAnalysis/ea-utils) and mapped to the *P. aeruginosa* PA14 genome (RefSeq accession GCF_000404265.1) using bowtie2[47]. FeatureCounts was used to assess the number of reads per gene[48]. Normalization and identification of significantly differentially regulated genes (FDR < 0.05, absolute $\log_2$ fold change (FC) > 1) was performed in R using the glmTreat-function of edgeR[49]. Cluster assignment of differentially expressed genes was performed with the package mfuzz[50].

Data availability

RNAseq raw data have been deposited at the NCBI gene expression omnibus database under accessions GSE159698 (https://www.ncbi.nlm.nih.gov/geo/query/acc.cgi?acc=GSE159698) and GSE217100 (https://www.ncbi.nlm.nih.gov/geo/query/acc.cgi?acc=GSE217100).

Acknowledgements

S.H. was funded by the Lower Saxony Ministry for Science and Culture (Bacdata ZN3428), the European Union (EU, ERC Consolidator Grant COMBAT 724290) and by the Deutsche Forschungsgemeinschaft (DFG, German Research Foundation) under Germany's Excellence Strategy (EXC 2155 390874280). Furthermore, S.H. received additional funding from the DFG (DFG SPP 1879) and the Novo Nordisk Foundation (NNF 18OC0033946). J.T. received funding from the mobility grant of the Czech Ministry of Education (CZ.02.2.69/0.0/0.0/18_053/0017705). The authors thank Astrid Dröge and Ina Schleicher for technical support.

References

1. Reyes-Lamothe R, Sherratt DJ. The bacterial cell cycle, chromosome inheritance and cell growth. *Nat Rev Microbiol*. 2019;17(8):467-478. doi:10.1038/s41579-019-0212-7
2. Couturier E, Rocha EPC. Replication-associated gene dosage effects shape the genomes of fast-growing bacteria but only for transcription and translation genes. *Molecular Microbiology*. 2006;59(5):1506-1518. doi:10.1111/j.1365-2958.2006.05046.x
3. Slager J, Veening JW. Hard-Wired Control of Bacterial Processes by Chromosomal Gene Location. *Trends in Microbiology*. 2016;24(10):788-800. doi:10.1016/j.tim.2016.06.003
4. Soler-Bistué A, Mondotte JA, Bland MJ, Val ME, Saleh MC, Mazel D. Genomic Location of the Major Ribosomal Protein Gene Locus Determines Vibrio cholerae Global Growth and Infectivity. *PLOS Genetics*. 2015;11(4):e1005156. doi:10.1371/journal.pgen.1005156
5. Narula J, Kuchina A, Lee D yeon D, Fujita M, Süel GM, Igoshin OA. Chromosomal Arrangement of Phosphorelay Genes Couples Sporulation and DNA Replication. *Cell*. 2015;162(2):328-337. doi:10.1016/j.cell.2015.06.012
6. Stokke C, Waldminghaus T, Skarstad K 2011. Replication patterns and organization of replication forks in Vibrio cholerae. *Microbiology*. 157(3):695-708. doi:10.1099/mic.0.045112-0
7. Quardokus EM, Brun YV. Cell cycle timing and developmental checkpoints in Caulobacter crescentus. *Current Opinion in Microbiology*. 2003;6(6):541-549. doi:10.1016/j.mib.2003.10.013
8. Nathwani D, Raman G, Sulham K, Gavaghan M, Menon V. Clinical and economic consequences of hospital-acquired resistant and multidrug-resistant Pseudomonas aeruginosa infections: a systematic review and meta-analysis. *Antimicrobial Resistance and Infection Control*. 2014;3(1):32. doi:10.1186/2047-2994-3-32
9. Rossi E, La Rosa R, Bartell JA, et al. Pseudomonas aeruginosa adaptation and evolution in patients with cystic fibrosis. *Nat Rev Microbiol*. 2021;19(5):331-342. doi:10.1038/s41579-020-00477-5
10. La Rosa R, Johansen HK, Molin S. Convergent Metabolic Specialization through Distinct Evolutionary Paths in Pseudomonas aeruginosa. *mBio*. 2018;9(2):e00269-18. doi:10.1128/mBio.00269-18
11. Gibson B, Wilson DJ, Feil E, Eyre-Walker A. The distribution of bacterial doubling times in the wild. *Proceedings of the Royal Society B: Biological Sciences*. 285(1880):20180789. doi:10.1098/rspb.2018.0789
12. Vallet-Gely I, Boccard F. Chromosomal Organization and Segregation in Pseudomonas aeruginosa. *PLOS Genetics*. 2013;9(5):e1003492. doi:10.1371/journal.pgen.1003492
13. Bhowmik BK, Clevenger AL, Zhao H, Rybenkov VV. Segregation but Not Replication of the Pseudomonas aeruginosa Chromosome Terminates at Dif. *mBio*. 2018;9(5):e01088-18. doi:10.1128/mBio.01088-18
14. Dötsch A, Schniederjans M, Khaledi A, et al. The Pseudomonas aeruginosa Transcriptional Landscape Is Shaped by Environmental Heterogeneity and Genetic Variation. *mBio*. 2015;6(4):e00749-15. doi:10.1128/mBio.00749-15
15. Tan J, Hammond JH, Hogan DA, Greene CS. ADAGE-Based Integration of Publicly Available Pseudomonas aeruginosa Gene Expression Data with Denoising Autoencoders Illuminates Microbe-Host Interactions. *mSystems*. 2016;1(1):e00025-15. doi:10.1128/mSystems.00025-15
16. Hornischer K, Khaledi A, Pohl S, et al. BACTOME—a reference database to explore the sequence- and gene expression-variation landscape of Pseudomonas aeruginosa clinical isolates. *Nucleic Acids Research*. 2019;47(D1):D716-D720. doi:10.1093/nar/gky895

17. Selim H, Radwan TEE, Reyad AM. Regulation of T3SS synthesis, assembly and secretion in Pseudomonas aeruginosa. *Arch Microbiol*. 2022;204(8):468. doi:10.1007/s00203-022-03068-5
18. Mesaros N, Glupczynski Y, Avrain L, Caceres NE, Tulkens PM, Van Bambeke F. A combined phenotypic and genotypic method for the detection of Mex efflux pumps in Pseudomonas aeruginosa. *Journal of Antimicrobial Chemotherapy*. 2007;59(3):378-386. doi:10.1093/jac/dkl504
19. Schuster M, Lostroh CP, Ogi T, Greenberg EP. Identification, Timing, and Signal Specificity of Pseudomonas aeruginosa Quorum-Controlled Genes: a Transcriptome Analysis. *Journal of Bacteriology*. 2003;185(7):2066-2079. doi:10.1128/JB.185.7.2066-2079.2003
20. Chadha J, Harjai K, Chhibber S. Revisiting the virulence hallmarks of Pseudomonas aeruginosa: a chronicle through the perspective of quorum sensing. *Environmental Microbiology*. 2022;24(6):2630-2656. doi:10.1111/1462-2920.15784
21. Díaz-Pérez AL, Zavala-Hernández AN, Cervantes C, Campos-García J. The gnyRDBHAL cluster is involved in acyclic isoprenoid degradation in Pseudomonas aeruginosa. *Appl Environ Microbiol*. 2004;70(9):5102-5110. doi:10.1128/AEM.70.9.5102-5110.2004
22. Herrick J, Sclavi B. Ribonucleotide reductase and the regulation of DNA replication: an old story and an ancient heritage. *Molecular Microbiology*. 2007;63(1):22-34. doi:10.1111/j.1365-2958.2006.05493.x
23. Margolin W. FtsZ and the division of prokaryotic cells and organelles. *Nat Rev Mol Cell Biol*. 2005;6(11):862-871. doi:10.1038/nrm1745
24. Mathee K, Narasimhan G, Valdes C, et al. Dynamics of Pseudomonas aeruginosa genome evolution. *Proceedings of the National Academy of Sciences*. 2008;105(8):3100-3105. doi:10.1073/pnas.0711982105
25. Sobetzko P, Travers A, Muskhelishvili G. Gene order and chromosome dynamics coordinate spatiotemporal gene expression during the bacterial growth cycle. *Proceedings of the National Academy of Sciences*. 2012;109(2):E42-E50. doi:10.1073/pnas.1108229109
26. Rossi E, Falcone M, Molin S, Johansen HK. High-resolution in situ transcriptomics of Pseudomonas aeruginosa unveils genotype independent patho-phenotypes in cystic fibrosis lungs. *Nat Commun*. 2018;9(1):3459. doi:10.1038/s41467-018-05944-5
27. Schulz S, Eckweiler D, Bielecka A, et al. Elucidation of Sigma Factor-Associated Networks in Pseudomonas aeruginosa Reveals a Modular Architecture with Limited and Function-Specific Crosstalk. *PLOS Pathogens*. 2015;11(3):e1004744. doi:10.1371/journal.ppat.1004744
28. Lato DF, Golding GB. Spatial Patterns of Gene Expression in Bacterial Genomes. *J Mol Evol*. 2020;88(6):510-520. doi:10.1007/s00239-020-09951-3
29. Tomasch J, Koppenhöfer S, Lang AS. Connection Between Chromosomal Location and Function of CtrA Phosphorelay Genes in Alphaproteobacteria. *Frontiers in Microbiology*. 2021;12. Accessed October 2, 2022. https://www.frontiersin.org/articles/10.3389/fmicb.2021.662907
30. Rattray JB, Thomas SA, Wang Y, et al. Bacterial Quorum Sensing Allows Graded and Bimodal Cellular Responses to Variations in Population Density. *mBio*. 2022;13(3):e00745-22. doi:10.1128/mbio.00745-22
31. Anetzberger C, Pirch T, Jung K. Heterogeneity in quorum sensing-regulated bioluminescence of Vibrio harveyi. *Molecular Microbiology*. 2009;73(2):267-277. doi:10.1111/j.1365-2958.2009.06768.x

32. Patzelt D, Wang H, Buchholz I, et al. You are what you talk: quorum sensing induces individual morphologies and cell division modes in Dinoroseobacter shibae. *ISME J*. 2013;7(12):2274-2286. doi:10.1038/ismej.2013.107
33. Reck M, Tomasch J, Wagner-Döbler I. The Alternative Sigma Factor SigX Controls Bacteriocin Synthesis and Competence, the Two Quorum Sensing Regulated Traits in Streptococcus mutans. *PLOS Genetics*. 2015;11(7):e1005353. doi:10.1371/journal.pgen.1005353
34. Kordes A, Preusse M, Willger SD, et al. Genetically diverse Pseudomonas aeruginosa populations display similar transcriptomic profiles in a cystic fibrosis explanted lung. *Nat Commun*. 2019;10(1):3397. doi:10.1038/s41467-019-11414-3
35. Jeske A, Arce-Rodriguez A, Thöming JG, Tomasch J, Häussler S. Evolution of biofilm-adapted gene expression profiles in lasR-deficient clinical Pseudomonas aeruginosa isolates. *npj Biofilms Microbiomes*. 2022;8(1):1-14. doi:10.1038/s41522-022-00268-1
36. Laub MT, McAdams HH, Feldblyum T, Fraser CM, Shapiro L. Global Analysis of the Genetic Network Controlling a Bacterial Cell Cycle. *Science*. 2000;290(5499):2144-2148. doi:10.1126/science.290.5499.2144
37. Waldbauer JR, Rodrigue S, Coleman ML, Chisholm SW. Transcriptome and Proteome Dynamics of a Light-Dark Synchronized Bacterial Cell Cycle. *PLOS ONE*. 2012;7(8):e43432. doi:10.1371/journal.pone.0043432
38. De Nisco NJ, Abo RP, Wu CM, Penterman J, Walker GC. Global analysis of cell cycle gene expression of the legume symbiont Sinorhizobium meliloti. *PNAS*. 2014;111(9):3217-3224. doi:10.1073/pnas.1400421111
39. Bandekar AC, Subedi S, Ioerger TR, Sassetti CM. Cell-Cycle-Associated Expression Patterns Predict Gene Function in Mycobacteria. *Current Biology*. 2020;30(20):3961-3971.e6. doi:10.1016/j.cub.2020.07.070
40. Pountain A, Jiang P, Podkowik M, Shopsin B, Torres VJ, Yanai I. A quantitative model for the transcriptional landscape of the bacterial cell cycle. Published online October 23, 2022:2022.10.22.513359. doi:10.1101/2022.10.22.513359
41. Teeseling MCF van, Thanbichler M. Generating asymmetry in a changing environment: cell cycle regulation in dimorphic alphaproteobacteria. *Biological Chemistry*. 2020;401(12):1349-1363. doi:10.1515/hsz-2020-0235
42. Liberati NT, Urbach JM, Miyata S, et al. An ordered, nonredundant library of Pseudomonas aeruginosa strain PA14 transposon insertion mutants. *Proceedings of the National Academy of Sciences*. 2006;103(8):2833-2838. doi:10.1073/pnas.0511100103
43. Van P, Jiang W, Gottardo R, Finak G. ggCyto: next generation open-source visualization software for cytometry. *Bioinformatics*. 2018;34(22):3951-3953. doi:10.1093/bioinformatics/bty441
44. Bense S, Witte J, Preuße M, et al. Pseudomonas aeruginosa post-translational responses to elevated c-di-GMP levels. *Molecular Microbiology*. 2022;117(5):1213-1226. doi:10.1111/mmi.14902
45. Avraham R, Haseley N, Fan A, Bloom-Ackermann Z, Livny J, Hung DT. A highly multiplexed and sensitive RNA-seq protocol for simultaneous analysis of host and pathogen transcriptomes. *Nat Protoc*. 2016;11(8):1477-1491. doi:10.1038/nprot.2016.090
46. Freiherr von Boeselager R, Pfeifer E, Frunzke J. Cytometry meets next-generation sequencing – RNA-Seq of sorted subpopulations reveals regional replication and iron-triggered prophage induction in Corynebacterium glutamicum. *Sci Rep*. 2018;8(1):14856. doi:10.1038/s41598-018-32997-9
47. Langmead B, Salzberg SL. Fast gapped-read alignment with Bowtie 2. *Nat Methods*. 2012;9(4):357-359. doi:10.1038/nmeth.1923

48. Liao Y, Smyth GK, Shi W. featureCounts: an efficient general purpose program for assigning sequence reads to genomic features. *Bioinformatics*. 2014;30(7):923-930. doi:10.1093/bioinformatics/btt656
49. Robinson MD, McCarthy DJ, Smyth GK. edgeR: a Bioconductor package for differential expression analysis of digital gene expression data. *Bioinformatics*. 2010;26(1):139-140. doi:10.1093/bioinformatics/btp616
50. Futschik ME, Carlisle B. Noise-robust soft clustering of gene expression time-course data. *J Bioinform Comput Biol*. 2005;03(04):965-988. doi:10.1142/S0219720005001375

Figure Legends

Figure 1. Growth and Replication dynamics of *P. aeruginosa* in LB medium. (A) Optical density and cell numbers followed for 10 h of growth in LB medium. **(B)** Distribution of cell area as determined from EM micrographs. **(C)** Distribution of chromosome content revealed by flow cytometric analysis of SybrGreen fluorescence (One to four chromosome equivalents indicated by color). The lower panel shows representative distributions of fluorescence intensity for up to 7 h. R indicates replicating cells during coupled growth. **(D)** Representative EM micrographs of cells during uncoupled (3 h) and coupled (10 h) growth. Visible division planes are marked by a white arrow.

Figure 2. Transcriptome dynamics during growth in LB medium. (A) Expression dynamics of the eight clusters determined with mfuzz. Shown are the changes of the average expression in the according clusters during the course of a 10h-cultivation. **(B)** Significantly ($p < 0.05$) enriched KEGG-categories in the eight clusters. Size indicates the number of enriched genes in the category, color is according to p-value.

Figure 3. Global chromosomal gene expression changes between different growth phases. (A) Distribution of genes on the chromosomes that show the highest expression during uncoupled (clusters 1-3), transition (clusters 4-6) and coupled (clusters 7-8) growth phases. **(B)** Expression of genes located in the ori and ter proximal during uncouples (1-3 h), transition (4-5 h) and coupled (6-10 h) growth phases. **(C)** $\log_2$ FCs between time points from different growth phases. Red lines show the fitted general additive models; orange lines show the models shifted up with the conserved region at the terminus set to $\log_2$ FC of zero. Representative chromosome content indicative for the different growth phases is shown on the right.

Figure 4. Transcriptomes of replicating and non-replicating cells during coupled growth. (A) Sampling scheme for method evaluation. **(B)** Correlation between transcriptomes of differently treated RNAs. Data for two additional replicates are shown in Supplementary Figure S4A. **(C)** Differential expression between replicating (R) and non-replicating (C1, C2) cells. Number of significantly up- and down-regulated genes between fractions (dark red) are shown in the left and right corner at the bottom of each panel, respectively. **(D)** Chromosome-wide differential gene expression in replicating (R) versus non-replicating (C1) cells. Genes that change significantly in expression are marked in dark red. Operons discussed in the text are marked in yellow. The cell-division gene cluster is shown above the plot. The red line shows a fitted general additive model. Data for the comparisons R vs. C2 and C2 vs. C1 is shown in Supplementary Figure S4B.

Supplementary Figure Legends

Supplementary Figure S1. Flow cytometric determination of relative cell size and chromosome content during growth in LB medium. (A) Changes of the side scatter (SSC) indicates reductive cell division from 3 h to 7 h cultivation time. **(B)** Changes in the distribution of chromosome content for three biological replicates in the course of 10 h cultivation.

Supplementary Figure S2. Transcriptome dynamics during growth in LB medium. (A) Multidimensional scaling (MDS) plot of samples taken during 10 h cultivation. Note the different timing during the shift to coupled growth (6 h sample) for the two independent experiments. **(B)** Determination of ideal number of clusters based on the minimum centroid distance within the clusters. Increasing the number of clusters above 8 does not lead to further reduction of centroid distance. **(C)** Expression profiles of genes in the 8 clusters determined with the mfuzz-package. The number of genes within the cluster is shown below the cluster number. Cluster affiliation alongside expression data is also documented in Supplementary Table S1.

Supplementary Figure S3. Time-resolved chromosomal gene expression changes during growth in LB medium. $\log_2$ fold changes between subsequent time points are shown. Red lines show the fitted general additive models.

Supplementary Figure S4. Transcriptomes of replicating and non-replicating cells during coupled growth. (A) Correlation between transcriptomes of differently treated RNAs (see Figure 4A). **(B)** Chromosome-wide differential gene expression in replicating pre-divisonal (C2) versus non-replicating (C1) and replicating (R) versus non-replicating cells. Genes that change significantly in expression are marked in dark red. The red line shows a fitted general additive model.

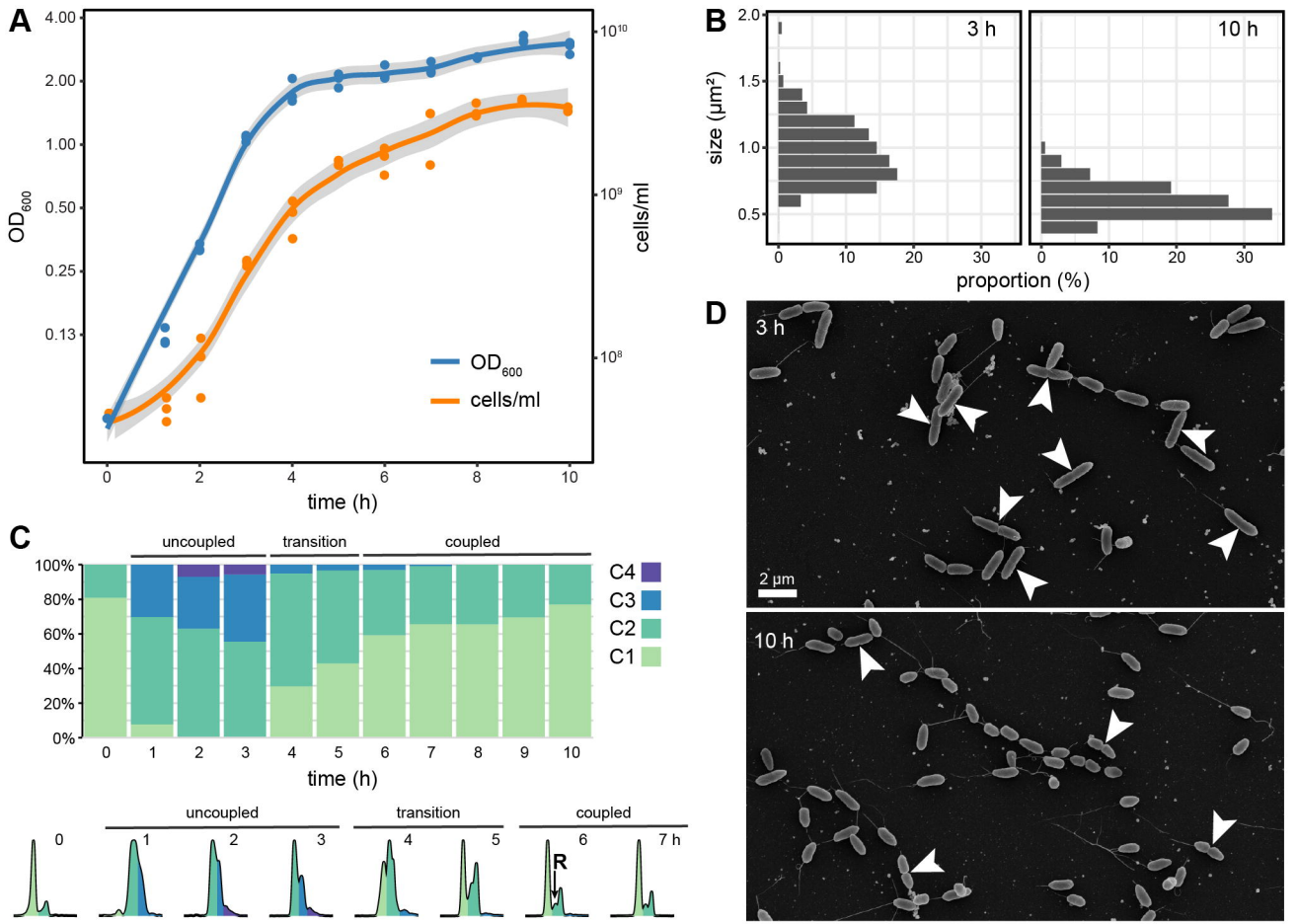
A
4.00
2.00
1.00
0.50
0.25
0.13
OD600
10^10
10^9
10^8
cells/ml
OD600
cells/ml
0
2
4
6
8
10
time (h)
B
3 h
10 h
size (µm²)
2.0
1.5
1.0
0.5
0
10
20
30
proportion (%)
C
uncoupled
transition
coupled
100%
80%
60%
40%
20%
0%
C4
C3
C2
C1
0
1
2
3
4
5
6
7
8
9
10
time (h)
uncoupled
transition
coupled
0
1
2
3
4
5
6
7 h
R
D
3 h
2 µm
10 h

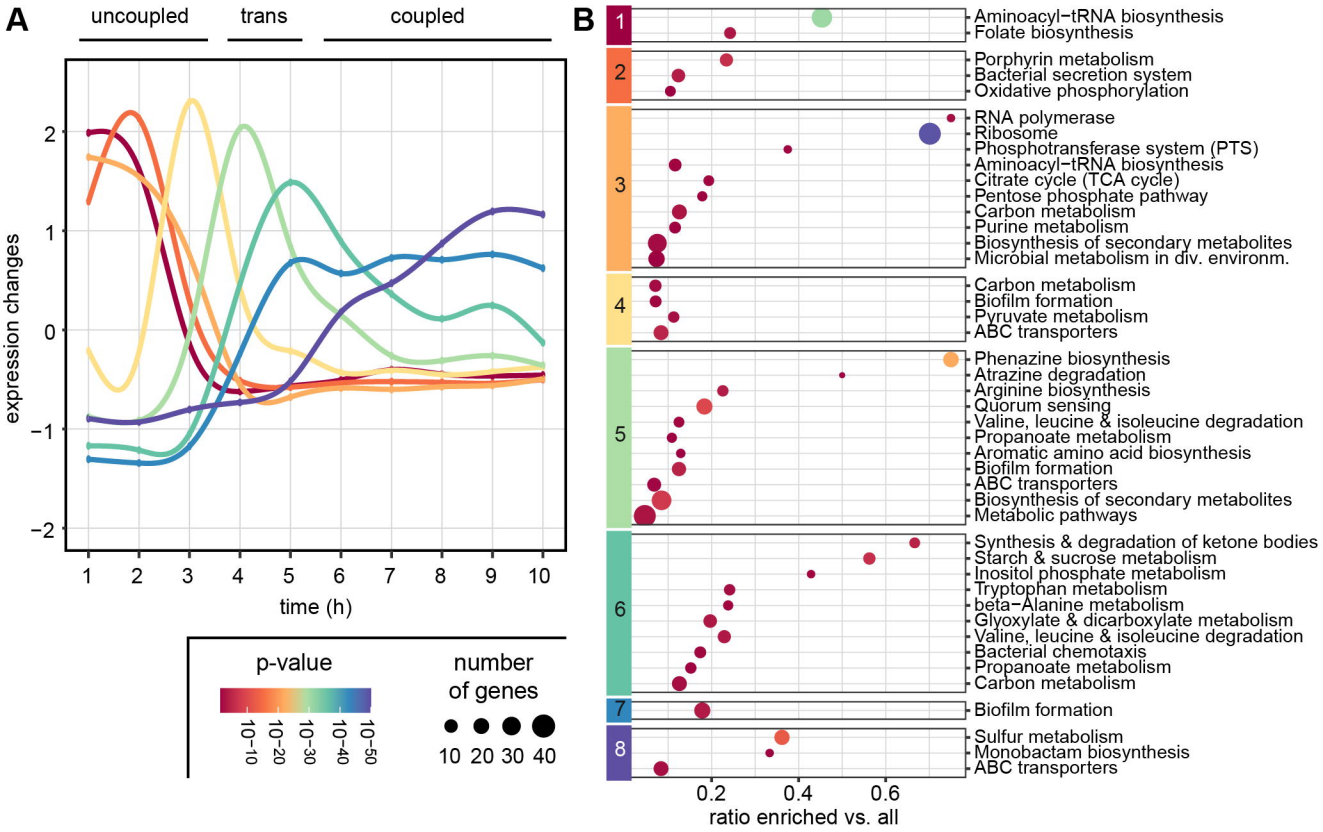
A
uncoupled
trans
coupled
expression changes
time (h)
p-value
number of genes
10 20 30 40
B
1
Aminoacyl−tRNA biosynthesis
Folate biosynthesis
2
Porphyrin metabolism
Bacterial secretion system
Oxidative phosphorylation
3
RNA polymerase
Ribosome
Phosphotransferase system (PTS)
Aminoacyl−tRNA biosynthesis
Citrate cycle (TCA cycle)
Pentose phosphate pathway
Carbon metabolism
Purine metabolism
Biosynthesis of secondary metabolites
Microbial metabolism in div. environm.
4
Carbon metabolism
Biofilm formation
Pyruvate metabolism
ABC transporters
5
Phenazine biosynthesis
Atrazine degradation
Arginine biosynthesis
Quorum sensing
Valine, leucine & isoleucine degradation
Propanoate metabolism
Aromatic amino acid biosynthesis
Biofilm formation
ABC transporters
Biosynthesis of secondary metabolites
Metabolic pathways
6
Synthesis & degradation of ketone bodies
Starch & sucrose metabolism
Inositol phosphate metabolism
Tryptophan metabolism
beta−Alanine metabolism
Glyoxylate & dicarboxylate metabolism
Valine, leucine & isoleucine degradation
Bacterial chemotaxis
Propanoate metabolism
Carbon metabolism
7
Biofilm formation
8
Sulfur metabolism
Monobactam biosynthesis
ABC transporters
ratio enriched vs. all

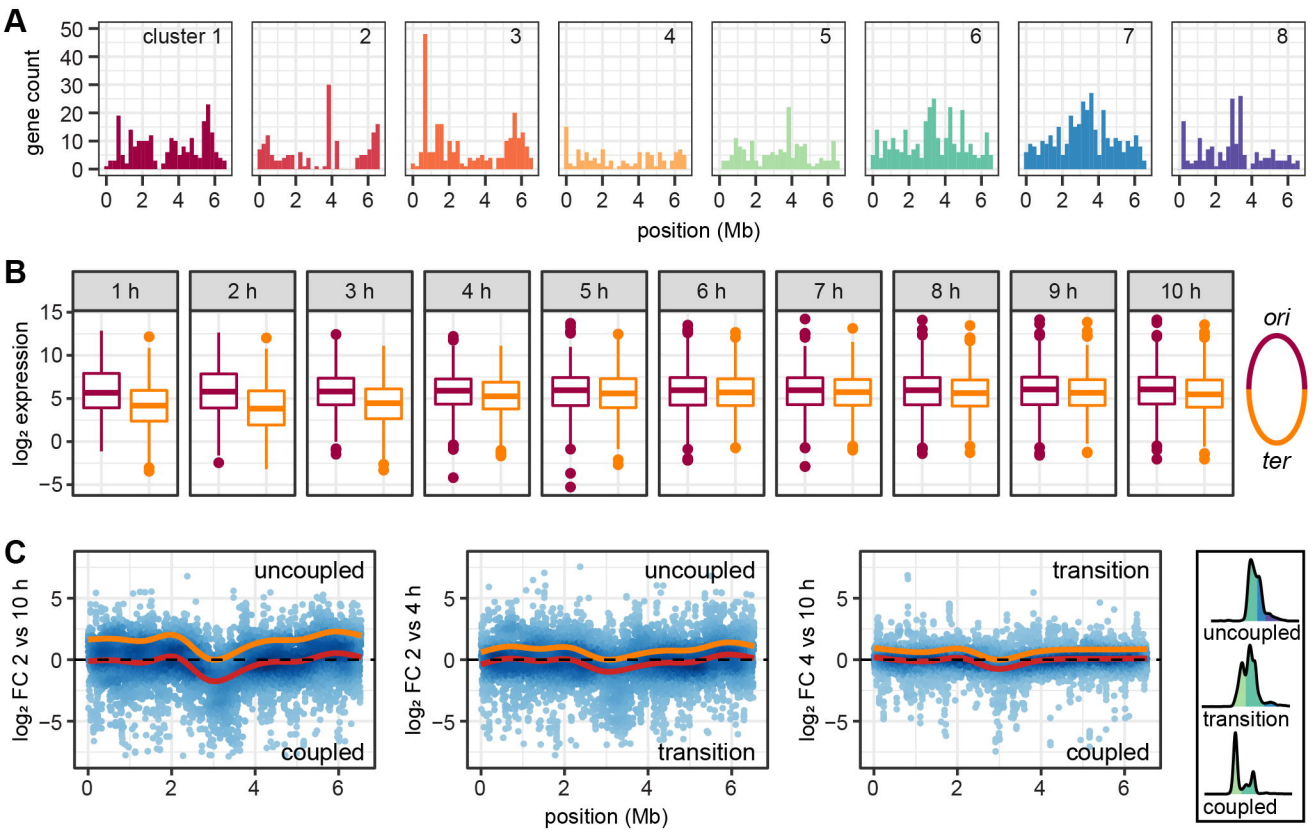
A
gene count
cluster 1
2
3
4
5
6
7
8
position (Mb)
B
1 h
2 h
3 h
4 h
5 h
6 h
7 h
8 h
9 h
10 h
log₂ expression
ori
ter
C
log₂ FC 2 vs 10 h
uncoupled
coupled
log₂ FC 2 vs 4 h
uncoupled
transition
log₂ FC 4 vs 10 h
transition
coupled
position (Mb)
uncoupled
transition
coupled

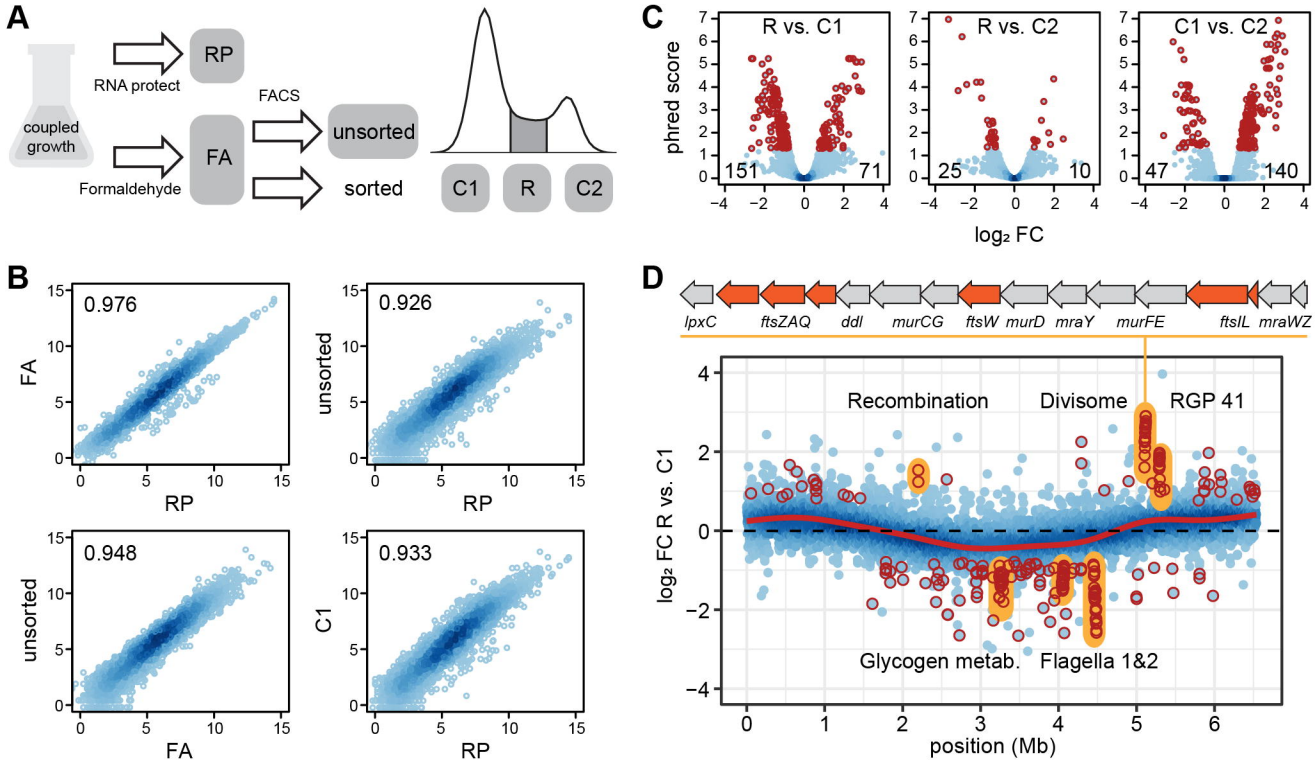
A
coupled growth
RNA protect
RP
Formaldehyde
FA
FACS
unsorted
sorted
C1
R
C2
B
0.976
FA
RP
0.926
unsorted
RP
0.948
unsorted
FA
0.933
C1
RP
C
R vs. C1
R vs. C2
C1 vs. C2
phred score
151
71
25
10
47
140
log2 FC
D
lpxC
ftsZAQ
ddl
murCG
ftsW
murD
mraY
murFE
ftsIL
mraWZ
Recombination
Divisome
RGP 41
Glycogen metab.
Flagella 1&2
log2 FC R vs. C1
position (Mb)